Molecular Vision 2014; 20:1109-1121 <http://www.molvis.org/molvis/v20/1109>
Received 12 December 2013 | Accepted 29 July 2014 | Published 31 July 2014

ERK1/2/COX-2/PGE_2 signaling pathway mediates GPR91-dependent VEGF release in streptozotocin-induced diabetes

Tingting Li,[1] Jianyan Hu,[1] Shanshan Du,[1] Yongdong Chen,[1] Shuai Wang,[1] Qiang Wu[1,2]

(The first two authors contributed equally to this work.)

[1]Department of Ophthalmology, the Sixth People's Hospital, Shanghai Jiaotong University, Shanghai, China; [2]Shanghai Key Laboratory of Diabetes Mellitus, Shanghai, China

Purpose: Retinal vascular dysfunction caused by vascular endothelial growth factor (VEGF) is the major pathological change that occurs in diabetic retinopathy (DR). It has recently been demonstrated that G protein-coupled receptor 91 (GPR91) plays a major role in both vasculature development and retinal angiogenesis. In this study, we examined the signaling pathways involved in GPR91-dependent VEGF release during the early stages of retinal vascular change in streptozotocin-induced diabetes.

Methods: Diabetic rats were assigned randomly to receive intravitreal injections of shRNA lentiviral particles targeting GPR91 (LV.shGPR91) or control particles (LV.shScrambled). Accumulation of succinate was assessed by gas chromatography-mass spectrometry (GC-MS). At 14 weeks, the ultrastructure and function of the retinal vessels of diabetic retinas with or without shRNA treatment were assessed using hematoxylin and eosin (HE) staining, transmission electron microscopy (TEM), and Evans blue dye permeability. The expression of GPR91, extracellular signal-regulated kinases 1 and 2 (ERK1/2) and cyclooxygenase-2 (COX-2) were measured using immunofluorescence and western blotting. COX-2 and VEGF mRNA were determined by quantitative RT–PCR. Prostaglandin E_2 (PGE_2) and VEGF secretion were detected using an enzyme-linked immunosorbent assay.

Results: Succinate exhibited abundant accumulation in diabetic rat retinas. The retinal telangiectatic vessels, basement membrane thickness, and Evans blue dye permeability were attenuated by treatment with GPR91 shRNA. In diabetic rats, knockdown of GPR91 inhibited the activities of ERK1/2 and COX-2 as well as the expression of PGE_2 and VEGF. Meanwhile, COX-2, PGE_2, and VEGF expression was inhibited by ERK1/2 inhibitor U0126 and COX-2 inhibitor NS-398.

Conclusions: Our data suggest that hyperglycemia causes succinate accumulation and GPR91 activity in retinal ganglion cells, which mediate VEGF-induced retinal vascular change via the ERK1/2/COX-2/PGE_2 pathway. This study highlights the signaling pathway as a potential target for intervention in DR.

Diabetes mellitus is characterized by hyperglycemia and a consequent functional failure of various target organs, including the eyes. Diabetic retinopathy (DR) is one of the fastest growing causes of blindness and visual impairment in the working-age population. The pathogenesis and development of DR are highly complex due to the involvement of multiple interlinked mechanisms. Various metabolic pathways triggered by hyperglycemia are involved, such as the polyol pathway, hexosamine pathway, and diacylglycerol (DAG)-protein kinase C (PKC) pathway [1]. In parallel, classically, oxidative stress [2], hemodynamic changes [3], and the production of free radicals, cytokines [4], or advanced glycosylation end-products [5] have also been considered to be crucial for the development of DR. However, the pathogenesis of DR has not been elucidated completely, despite much investigation.

Correspondence to: Qiang Wu, Department of Ophthalmology, The Sixth People's Hospital, Shanghai Jiaotong University, 600 Yishan Road, Shanghai 200233, China. Phone: +86-18930177422; FAX: +86-021-64701361; email: Qiang.wu@shsmu.edu.cn

Vascular endothelial growth factor (VEGF) has been recognized as the prominent mediator in the process of DR, and overexpression of VEGF is believed to correlate with the vascular hyperpermeability and neovascularization in diabetic subjects [6]. Because vascular supply is tightly coupled to tissue metabolic rate, it is conceivable that energy source metabolic intermediates also affect the progression of DR [7]. Succinate, a Krebs cycle intermediate normally found in mitochondria, is released into the extracellular medium if the local tissue energy demand and supply are imbalanced [8]. Local accumulation of succinate is recognized as an indicator of diabetic organ damage [9,10]. Most recently, it has been suggested that high levels of succinate were detected in patients with proliferative diabetic retinopathy (PDR) [11]. G protein-coupled receptor 91 (GPR91), a known specific receptor for succinate, is expressed in the kidney, spleen, placenta, liver, and retina [7]. It has been demonstrated that GPR91 plays a critical role in the pathogenesis of diabetic neuropathy, hypertension, heart stress, and liver damage [9,12-14]. Sapieha et al. has found that GPR91 plays a major

role in the settings of both normal retinal development and proliferative ischemic retinopathy [7]. We previously assessed the role of GPR91 in high-glucose-induced VEGF release in vitro [15]. Nevertheless, the influence of GPR91 on retinal vascular dysfunction in DR and the underlying molecular mechanisms remain unknown. Unveiling these precise mechanisms may contribute to clarifying the pathogenesis of DR.

DR is a multifactorial disease in which a variety of signaling pathways and active substances are involved. Cyclooxygenase-2 (COX-2) and COX-2-induced prostaglandin E_2 (PGE_2) have been confirmed to participate in this process and regulate the expression of VEGF [16]. In addition, extracellular signal-regulated kinases 1 and 2 (ERK1/2), a major subfamily of mitogen-activated protein kinase (MAPK) signaling, is recognized as an important pathway in the transduction of extracellular signals to cellular responses and is involved in various physiologic effects and pathological processes [17,18]. ERK1/2 has been verified to mediate VEGF release in oncoma and hematologic diseases [19,20]. The overwhelming majority of research verifies that the ERK1/2 signaling pathway plays a key role in the occurrence and development of DR [21,22]. Recently, one study of diabetic nephropathy showed that accumulating succinate under hyperglycemia conditions induced ERK1/2 activation, COX-2, and PGE_2 upregulation by binding with activated GPR91 [10,23].

In this study, we constructed a lentiviral expression vector containing a GPR91 shRNA and used it to investigate the role of GPR91 in VEGF release and to dissect the potential molecular mechanisms involved in DR. We examined the hypothesis that the ERK1/2/COX-2/PGE_2 signaling pathway mediates GPR91-dependent VEGF release during the early stages of retinal vascular dysfunction in a streptozotocin (STZ)-induced diabetic model.

METHODS

Animals: Male Sprague-Dawley (SD) rats (2 months old, 200–250 g) were purchased from the SIPPR/BK Lab Animal Ltd (Shanghai, China). The rats were housed in a barrier facility with free access to normal food and tap water. They were maintained under conditions of standard lighting (a 12 h:12 h light-dark cycle), temperature (23–25 °C), and humidity (50%–60%). Diabetes was induced using STZ based on a previously published protocol [24]. The rats were injected with a single intraperitoneal dose of 60 mg/kg STZ in 100 mM citrate buffer (pH 4.5). Weight- and age-matched non-diabetic control rats received injections of an equal volume of citrate buffer. Following STZ injection (48 h post-injection), a blood sample was taken from the tail vein of each rat, and the blood glucose level was measured using an automatic analyzer (Optium Xceed, Abbott Diabetes Care, Bedford, MA). The maintenance of a diabetic state was confirmed by weekly tail vein-blood glucose measurements. Animals with plasma glucose concentrations >16.7 mmol/l were deemed diabetic and were included in the study. Treatment of the animals conformed to the Guide for Care and Use of Laboratory Animals published by the National Institutes of Health (Guide for the Care and Use of Laboratory Animals, 1996), and the protocols were approved by the Animal Ethics Committee of the Sixth People's Hospital, Shanghai Jiaotong University.

The recombinant GPR91 shRNA (AACCCTAAATACAGTCTCATT) and the scrambled shRNA were designed and packaged by Genechem Co., Ltd (Shanghai, China), as described previously [15]. DNA oligos containing the target sequence were chemically synthesized, annealed, and inserted into the lentivirus expression vector pGCSIL-GFP by double digestion with AgeI and EcoRI and ligation with T4 DNA ligase. The ligate was transformed into competent Escherichia coli DH5α cells. Restriction enzyme analysis and DNA sequencing were used to identify the desired transformants. The lentivirus carrying GPR91 shRNA was produced by plasmid cotransfection of 293T cells. The viral supernatant was collected after transfection for 48 h, passed through 0.45-mm filters, concentrated and titered to 10^9 TU/ml (transfection unit). The rats were randomized into six groups and treated as follows: (1) control group, non-diabetic rats; (2) STZ group, diabetic rats not treated with the lentiviral particle; (3) LV.shScrambled group, diabetic rats that received an intravitreal injection of the scrambled shRNA lentiviral particles (1 µl, 1×10^8 TU/ml) 2 weeks after the induction of diabetes; (4) LV.shGPR91 group, diabetic rats that received an intravitreal injection of the GPR91 shRNA lentiviral particles (1 µl, 1×10^8 TU/ml) 2 weeks after the induction of diabetes; (5) U0126 group, diabetic rats that received an intravitreal injection of 0.1 mM U0126 (ERK1/2 inhibitor, Calbiochem, Gibbstown, NJ) before the diabetic model was induced; and (6) NS-398 group, diabetic rats that received an intravitreal injection of 0.5 mM NS-398 (COX-2 inhibitor, Cayman, Ann Arbor, MI) before the diabetic model was induced.

Gas chromatography-mass spectrometry analysis: Retinal samples were freshly harvested and homogenized ultrasonically for 4 min. Next, 3 µl 2,2,3,3-^{2}H4-succinic acid (CDN Isotopes, Pointe-Claire, Canada) was added to each tissue sample as an internal standard in water, and an additional 200 µl water was added according to the reported protocol [7]. Briefly, 150 µl methanol and 50 µl chloroform were added

and the mixture was centrifuged at 3600 ×g for 10 min. The clear supernatants were collected, and nitrogen and 80 µl methoxamine (15 mg/ml) were added to the dried samples. The samples were incubated overnight and Bis-trimethylsilyl-trifluoroacetamide (BSTFA) was added to the reaction samples. They were concentrated for 1.5 h and prepared for GC/MS analysis (Comprehensive Two-dimensional Gas Chromatography/Time-of-flight Mass Spectrometer, Pegasus 4D GC×GC-TOFMS, Leco, St. Joseph, MI).

Hematoxylin and eosin staining and quantification of blood vessels: The fixed eyes were processed routinely and embedded in paraffin wax. Paraffin-embedded retinal sections (5 µm) were dewaxed and dehydrated. The sections were taken at approximately 100 µm intervals and spanned the entire retina. For each eye, three sections were randomly chosen and evaluated. An average of 15 to 18 sections for each group was assessed. The sections stained using hematoxylin and eosin (HE) were analyzed and photographed by the same examiner, who was blinded to the source of the tissue, using a light microscope equipped with a camera (Leica, Wetzlar, Germany). The retinal areas in each image that were used to calculate the number of blood vessel profiles (BVPs) in the inner retina were chosen according to a previous study [25]. Briefly, we divided 180×110 mm area into 16-U areas for each image. An automatic stage produced an unbiased counting frame to advance across the entire retina.

Immunofluorescence: Retinal sections were blocked in 5% BSA for 1 h at room temperature, followed by incubation with retinal ganglion cell (RGC) specific marker γ-synuclein (1:50, Santa Cruz, Dallas, TX), endothelial-cell specific marker isolectin B4(1:50, Santa Cruz, CA), GPR91 (1:50, Novus Biologicals, Littleton, CO), p-ERK1/2 (1:50, Cell Signaling Technology, Boston, MA), and COX-2 (1:50, Santa Cruz, CA) primary antibodies overnight at 4 °C. The retinal sections then were incubated in CY3-conjugated anti-rabbit and FITC-conjugated anti-mouse secondary antibodies (1:200, Invitrogen, Carlsbad, CA) for 1 h at room temperature. Fluorescence image capture and analysis were performed with a fluorescence microscope (Leica, Wetzlar, Germany).

Transmission electron microscopy: Rat retinas were fixed in 2.5% glutaraldehyde and post-fixed in 1% osmium tetroxide after dissection out of four random areas from the central and peripheral retina. The specimens were then embedded in Spurr resin. The tissue blocks were orientated using 1 µm sections stained with toluidine blue, and the ultrathin sections were contrasted using uranyl acetate and lead citrate before examination using transmission electron microscopy (TEM) (CM-120, Philips, Eindhoven, Netherlands). Computer-assisted morphometric measurements were used by AxioVision 4.8 software.

Measurement of retinal vascular leakage using Evans blue dye: Retinal vascular leakage was quantitated using Evans blue dye according to the standard protocol [26]. Briefly, the right iliac vein and iliac artery were cannulated using polyethylene tubing, and Evans blue was injected through the iliac vein at a dosage of 45 mg/kg. Blood (100 µl) was withdrawn from the iliac artery in 15-min intervals. After the dye had circulated for 120 min, the animal was perfused through the left ventricle using citrate buffer (0.05 M, pH 3.5, 37 °C) for 2 min at 66 ml/min. Immediately after perfusion, both eyes were enucleated and the leakage of Evans blue dye was extracted from the retinas and was determined using the formula: (retinal Evans blue in micrograms/retina dry weight in grams) / (time-averaged plasma Evans blue in micrograms/plasma volume in microliters × circulation time in hours) [27].

Quantitative real-time PCR: After the rats were injected with a single intraperitoneal in dose of 50 mg/kg 2% pentobarbital sodium solution to euthanasia, each retina was dissected and frozen immediately in liquid nitrogen. The total RNA was extracted from neural retinal samples using Trizol reagent (Invitrogen). The primer sequences used were as follows: rat VEGF (forward: 5′-AAA GCC AGC ACA TAG GAG AG-3′; reverse: 5′-AGG ATT TAA ACC GGG ATT TC-3′), COX-2 (forward: 5′-TAC AAC AAC TCC ATC CTC CTT G-3′; reverse: 5′-TTC ATC TCT CTG CTC TGG TCA A-3′) and rat β-actin (forward: 5′-CAC CCG CGA GTA CAA CCT TC-3′; reverse: 5′-CCC ATA CCC ACC ATC ACA CC-3′). Quantitative real-time PCR was then performed using the SYBR Green qPCR Super Mixture (Takara, Tokyo, Japan) and an ABI Prism 7500 Sequence Detection System. All reactions were performed in triplicate. The data were analyzed using the $2^{-\square\square CT}$ method.

Western blot analysis: For the western blot analysis, the neural retinas were rapidly dissected from the euthanatized rats and lysed in RIPA buffer (Beyotime, Shanghai, China) containing a protease inhibitor (Beyotime, Shanghai, China) and phosphatase inhibitor (Roche, Mannheim, Germany). Aliquots containing 30 µg of protein were separated by SDS-polyacrylamide gel electrophoresis using a 10% gel, and the separated proteins were blotted onto PVDF membranes (Millipore, Billerica, MA) in a wet transfer unit (Bio-Rad, Hercules, CA). After blocking with 5% non-fat dry milk at room temperature for 1 h, the membranes were incubated overnight at 4°C with the following primary antibodies: GPR91 (1:1000), p-ERK1/2 (1:3000) , t-ERK1/2 (1:3000) , COX-2 (1:200), anti-VEGF (1:200, Abcam, Cambridge, MA) andβ-actin (1:1000, Abcam). After being washed with

TBS-Tween 20, the membranes were incubated with the appropriate HRP-conjugated secondary antibodies (1:1000, ProteinTech Group, Chicago, IL) for 1 h at room temperature. The bands were visualized using an enhanced ECL detection kit (Pierce Biothechnology, Rockford, IL). For the ELISA, the vitreous fluid samples were collected from rat eye for enzyme-linked immunosorbent assay analysis using kits from R&D Systems (Minneapolis, MN) following the instructions provided by the manufacturer.

Statistical analysis: All data are presented as the mean± standard deviation (SD). The data were analyzed using SPSS 16.0 software. The differences between multiple groups were assessed by one-way ANOVA, followed by Student–Newman–Keuls (SNK) comparisons. $p<0.05$ was considered statistically significant.

RESULTS

Succinate was increased in diabetic rat retinas and GPR91 was primarily located in retinal ganglion cells: The results of gas chromatography-mass spectrometry analysis indicated that the levels of succinate were markedly increased in fresh retinal samples from diabetic rats compared with non-diabetic retinas ($p<0.01$, Figure 1A). However, the expression of GPR91 did not change significantly between the non-diabetic and diabetic rat retinas ($p>0.05$, Figure 1B,C). Immunofluorescence showed that GPR91 was predominantly localized to the cell bodies of the ganglion cell layer (GCL) and to a lesser extent to cells of the inner nuclear layer (INL) and retinal pigment epithelium (RPE; Figure 1D). However, the endothelial cells did not express GPR91 (Figure 1E).

We then researched the expression of GPR91 using a shRNA approach in the retina. The retinal GPR91 level was significantly reduced in rats transduced with LV.shGPR91 compared with tissues from those transduced with LV.shScrambled at 4 weeks ($p<0.01$, Figure 1D,F,G).

In addition, we found that the nonfasting blood glucose was markedly higher in the diabetic rats than in the non-diabetic rats ($p<0.01$, Figure 1H), and local GPR91 knockdown produced no effect on hyperglycemia in the diabetic rats ($p>0.05$, Figure 1H). The bodyweights of the diabetic rats were significantly lower than that of the non-diabetic rats ($p<0.01$, Figure 1I).

Knockdown of GPR91 attenuated retinal vessel damage in diabetic rats: Pathological damage to the retinal vessel occurred in the 14 week STZ-induced diabetic rats (Figure 2). Compared with the non-diabetic rats, HE staining revealed that the retina tissue developed telangiectatic vessels in the inner layer of retinas (*black arrow* in Figure 2A), and the cells of the inner nuclear layer appeared to be disorder. The number of BVPs in the inner retina was increased (Figure 2B). TEM examination revealed that swelling was observed in the mitochondria of the pericytes and endothelial cells, and the mitochondrial membrane was ruptured (*white square frame* in Figure 2C). It was also demonstrated that the basement membrane thickness (BMT) was significantly greater in the diabetic retinal capillary ($p<0.01$, *black arrow* in Figure 2C,D). Furthermore, at the completion of the experiment, an increase in retinal vascular permeability was detected in diabetic rats ($p<0.01$, Figure 2E). Treatment with GPR91 shRNA attenuated the retinal vascular dysfunction and significantly decreased the BMT and Evans blue dye permeability ($p<0.01$, Figure 2A-E), whereas LV.shScrambled had no such effect ($p>0.05$, Figure 2D,E), and the damage to the inner nuclear layer was not attenuated in the GPR91 siRNA group (Figure 2A).

Effect of GPR91 on VEGF expression in the retinas of STZ-induced diabetic rats: Next, we sought to investigate the role of GPR91 in regulating VEGF secretion and retinal vascular damage in diabetic retinas. The retinal expression of VEGF was increased in diabetic rats in the 4 week experiment compared with non-diabetic rats (mRNA = 1.2:1; protein = 7.8:1), and the change in protein level was dramatic ($p<0.01$, Figure 2F,G). Furthermore, GPR91 knockdown reduced VEGF mRNA by approximately 25% in the STZ-induced diabetic rats ($p<0.05$, Figure 2F) and significantly decreased VEGF protein expression by approximately 75% ($p<0.01$, Figure 2G).

GPR91 modulated ERK1/2 signaling activity in diabetic rats: To confirm the presence and importance of the ERK1/2 signaling pathway in GPR91-dependent retinal vascular change in diabetic rats, we evaluated ERK1/2 activation in the retinas of diabetic rats transduced with LV.shScrambled or LV. shGPR91 compared with non-diabetic rats. Western blotting showed upregulation of ERK1/2 phosphorylation in the retinas of diabetic rats at 1 week and 2 weeks after the induction of diabetes and displayed a time-dependent trend (Figure 3A,B). Double immunofluorescence showed that the expression of ERK1/2 phosphorylation was increased in RGCs after STZ injection for 1 week (Figure 3C). However, the increases in p-ERK1/2 expression were significantly blocked by GPR91 shRNA ($p<0.01$, Figure 3D,E).

GPR91 modulated VEGF secretion via ERK1/2/COX-2/PGE_2 signaling pathway in diabetic rats: We then investigated the COX-2 and PGE_2 expression and the relationship among GPR91, ERK1/2, COX-2, and PGE_2 in the retinas of STZ-induced diabetic rats. The levels of COX-2 protein were increased during the period of 2 weeks to 6 weeks after

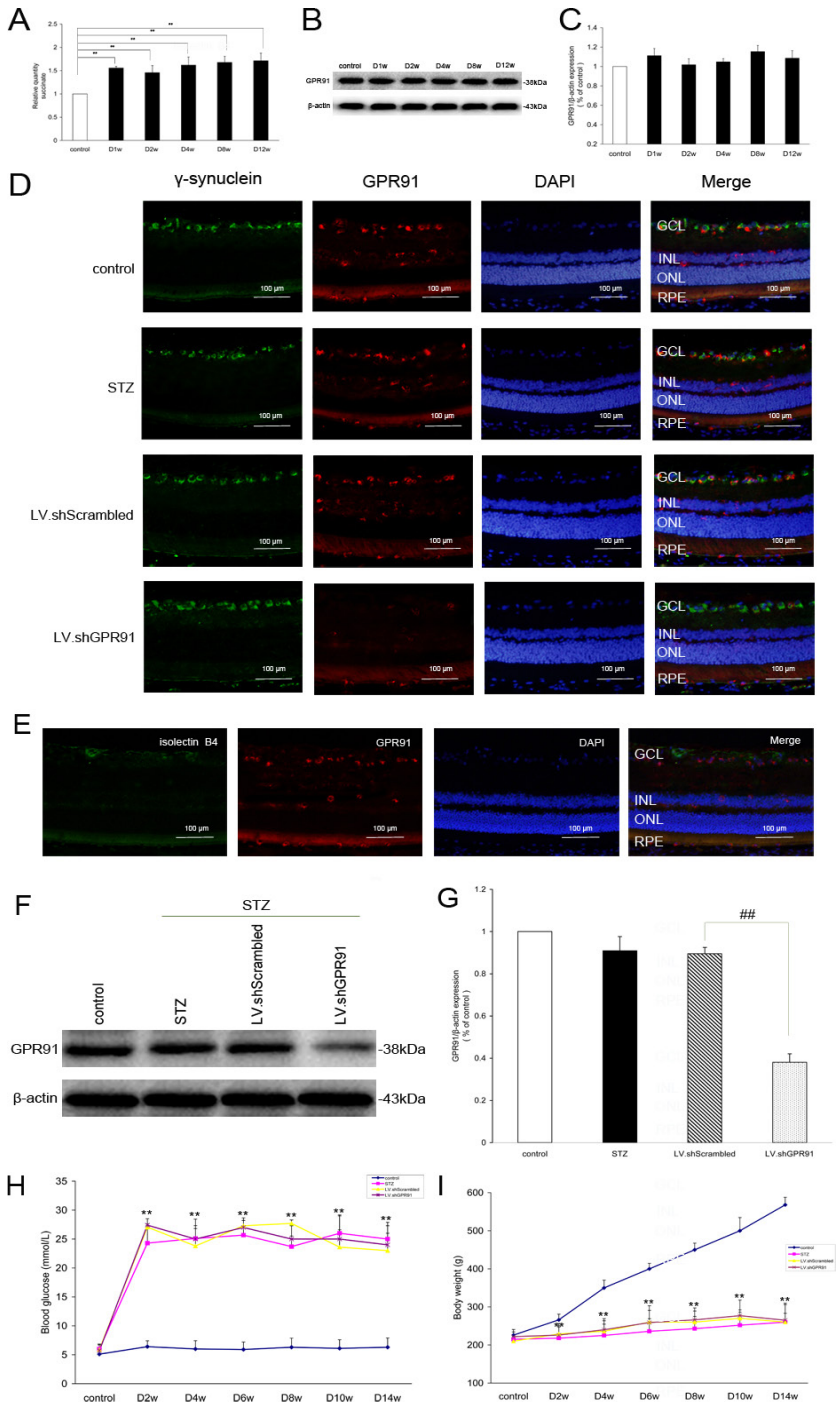

Figure 1. Succinate was increased in streptozotocin (STZ)-induced diabetic rats, and G protein-coupled receptor 91 (GPR91) was predominantly increased in retinal ganglion cells (RGCs). **A**: Retinal levels of succinate were detected by gas chromatography-mass spectrometry (GC-MS) analysis in non-diabetic rats and diabetic rats at 1 week, 2 week, 4 week, 8 week, and 12 week after STZ injection. The levels of succinate were markedly increased in fresh retinal samples from diabetic rats compared with non-diabetic retinas. Each column denotes the mean ± standard deviation (SD; n = 6). **B**: Western blot analysis of the GPR91 protein in samples from each group. **C**: The expression of GPR91 did not change significantly between the non-diabetic and diabetic rat retinas. Each column denotes the mean ± SD (n = 6). **D**: Immunofluorescence localization of GPR91 in the retina showing pronounced expression in the ganglion cell layer, and to a lesser extent, to cells of the inner nuclear layer and retinal pigment epithelium. GPR91 protein levels were significantly downregulated in rats transduced with GPR91 shRNA lentiviral particles compared to those transduced with the scrambled shRNA. GCL, ganglion cell layer; INL, inner nuclear layer; ONL, outer nuclear layer; RPE, retinal pigment epithelium. Scale bar, 100 μm. **E**: The immunofluorescence localization of GPR91 in the retina was not consistent with an endothelial cell. Scale bar, 100 μm. **F**: Western blot analysis of the GPR91 protein in samples from each group. Four week diabetic rats were treated with scrambled shRNA lentiviral particles or GPR91 shRNA lentiviral particles intravitreally. **G**: GPR91 protein levels were significantly downregulated in rats transduced with GPR91 shRNA lentiviral particles compared to those transduced with the scrambled shRNA. Each column denotes the mean ± SD (n = 6). **H**: The nonfasting blood glucose was detected in the 2 week to 14 week diabetic rats and non-diabetic rats. The nonfasting blood glucose was markedly higher in the diabetic rats than in the non-diabetic rats, and local GPR91 knockdown produced no effect on hyperglycemia in diabetic rats. Each node denotes the mean ± SD (n = 6). **I**: The bodyweights were recorded in the same period (from 2 week to 14 week) for the diabetic rats and non-diabetic rats. The bodyweights were significantly lower in the diabetic rats than the non-diabetic rats. Each node denotes the mean ± SD (n = 6). **p<0.01 versus control. ##p<0.01 versus LV.shScrambled group rats.

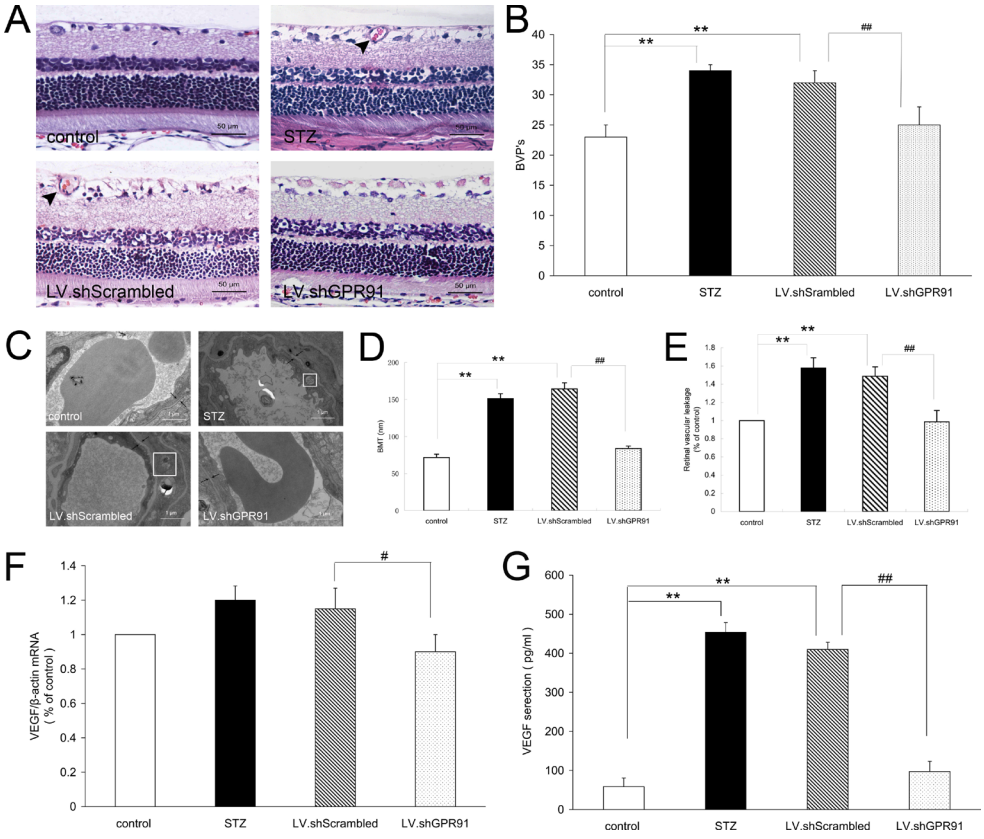

Figure 2. Attenuation of retinal vascular dysfunction and inhibition of vascular endothelial growth factor (VEGF) expression in STZ-induced diabetic rats following intravitreal injection of shRNA lentiviral particles targeting GPR91 (LV.shGPR91) particles. **A**: Light microscopy analysis of retinas from animals in each group. Compared with the non-diabetic rats, hematoxylin and eosin (HE) staining revealed that the retina tissue developed telangiectatic vessels in the inner layer of retinas and the irregular arrangement of cells in the inner nuclear layer in diabetic rats for the 14 week experiment. Treatment with GPR91 shRNA attenuated the retinal vascular dysfunction compare to LV.shScrambled group rats but had no effect on the damage of the inner nuclear layer. The *black arrows* indicate the telangiectatic vessel. Scale bar, 50 µm. **B**: The number of blood vessel profiles (BVPs) per unit area of the inner retina was increased in the 14 week diabetic rats compared with the non-diabetic rats. Treatment with GPR91 shRNA reduced the number of BVPs per unit area of the inner retina compared to rats in the LV.shScrambled group. Each column denotes the mean ± SD (n = 6). **C**: Transmission electron micrograph (TEM) images of the retinal microvasculature in samples from each group. TEM examinations revealed that swelling was observed in the mitochondria of the pericytes and endothelial cells and that the mitochondrial membrane was ruptured in the 14 week diabetic rats. Treatment with GPR91 shRNA significantly attenuated ultrastructural changes of the retina compared to the LV.shScrambled group rats. The *black arrow* denotes the segment of the outer capillary basement membrane between the endothelial cells and glia limitans, which was used to measure the basement membrane thickness. The *white square frame* denotes swelling in the mitochondria of the vascular pericytes and endothelial cells. Scale bar, 1 µm. **D**: In the 14 week diabetic retinal capillary, the basement membrane thickness (BMT) was significantly greater compared with the non-diabetic rats. Treatment with GPR91 shRNA significantly decreased the BMT compared to the LV.shScrambled group rats. Each column denotes the mean ± SD (n = 6). **E**: An increase in retinal vascular permeability was detected by Evans blue dye in the diabetic rats at the completion of the experiment. Treatment with GPR91 shRNA significantly reduced Evans blue dye permeability compared with the scrambled shRNA group. Each column denotes the mean ± SD (n = 6). **F**: qRT-PCR analysis for VEGF mRNA in the 4 week diabetic rat retinas was significantly upregulated compared with the non-diabetic rats. The levels of VEGF mRNA in the 4 week STZ rats treated with GPR91 shRNA were reduced by approximately 25% compared with the scrambled shRNA group. Each column denotes the mean ± SD (n = 6). **G**: Enzyme-linked immunosorbent assay analysis of vitreal VEGF release in vitreous. The retinal expression of VEGF protein was increased in diabetic rats for the 4 week experiment compared with the non-diabetic rats. GPR91 knockdown significantly reduced VEGF protein expression by approximately 75% compared with the scrambled shRNA group. Each column denotes the mean ± SD (n = 6). **p<0.01 versus control. #p<0.05 versus LV.shScrambled group rats. ##p<0.01 versus LV.shScrambled group rats.

the induction of diabetes (Figure 4A,B). The COX-2 expression located in RGCs was also enhanced (Figure 4C). PGE_2, measured because the production of PGE_2 denotes activity of COX-2, was also markedly increased in the retinas of diabetic rats at 4 weeks (p<0.01, Figure 4G). Furthermore, intravitreal injection of 0.1 mM U0126 or 0.5 mM NS-398 significantly blocked the upregulation of COX-2, PGE_2, and VEGF release (p<0.01, Figure 4D-I). These findings indicate that the ERK1/2 pathway is upstream of the COX-2/PGE_2 pathway, and the ERK1/2/COX-2/PGE_2 pathway is associated with VEGF release.

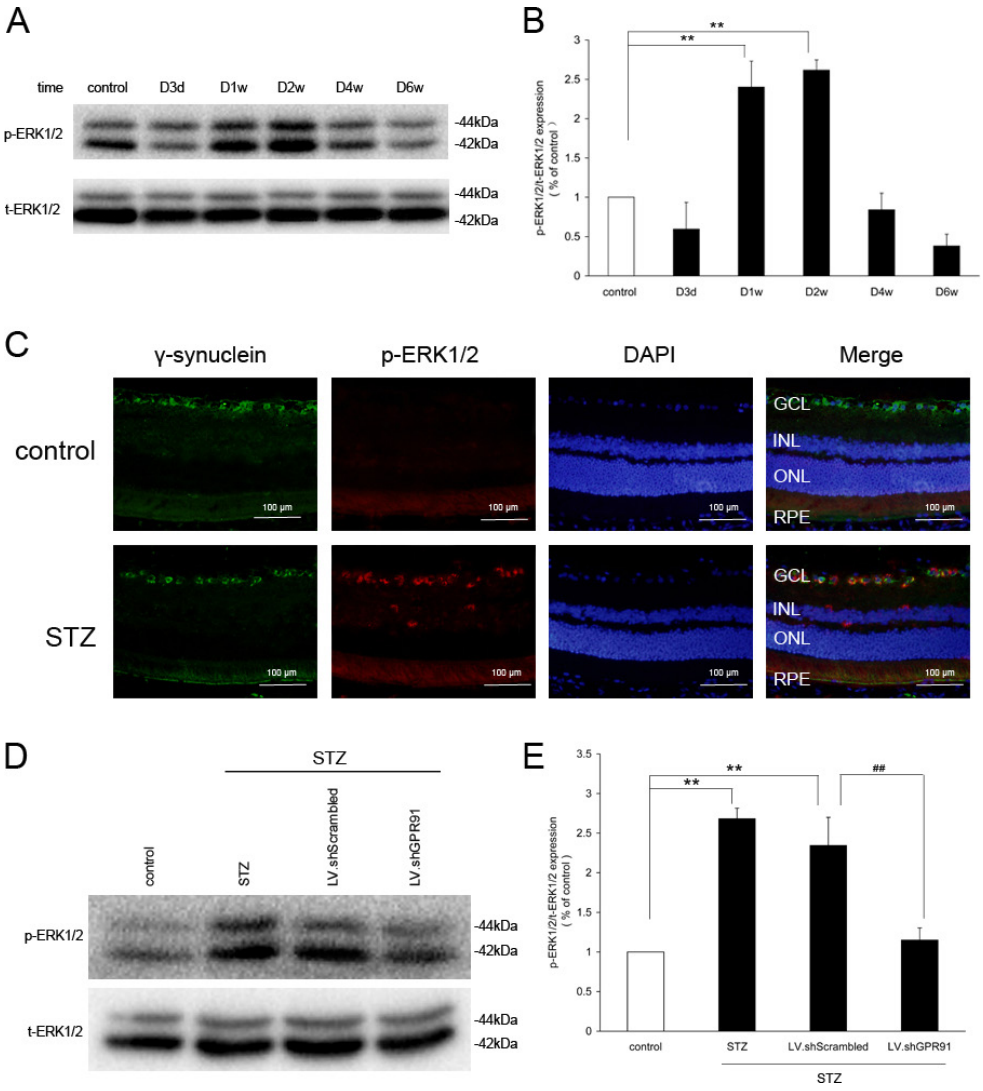

Figure 3. Activation of extracellular signal-regulated kinases 1 and 2 (ERK1/2) signaling pathways in the retinas of STZ rats. **A**: Western blot analysis of the ERK1/2 phosphorylation in the retinas of diabetic rats from 3 days to 6 weeks after the induction of diabetes. **B**: The levels of ERK1/2 phosphorylation were increased in the retinas of diabetic rats at 1 week and 2 weeks after the induction of diabetes and displayed a time-dependent trend. Each column denotes the mean ± SD (n = 6). **C**: Immunofluorescence showed that ERK1/2 expression located in the retinal ganglion cell layer increased in 1 week diabetic rats compared with control. Scale bar, 100 μm. **D**: Changes in ERK1/2 phosphorylation in the retinas of STZ rats transduced with LV.shScrambled or LV.shGPR91 using western blotting. Rats were analyzed after 1 week after the induction of diabetes. **E**: The increases in p-ERK1/2 expression were significantly blocked by GPR91 shRNA in the 1 week diabetic rats. Each column denotes the mean ± SD (n = 6). **p<0.01 versus control. ##p<0.01 versus LV.shScrambled group rats.

DISCUSSION

In the retina, VEGF is expressed in retinal ganglion cells, Müller cells, endothelial cells, astrocytes, and RPE [28]. Wang et al. [28] investigated the role of Müller cell-derived VEGF in retinal vascular leakage during the process of DR. Recent research found that GPR91 existed primarily in RGCs and that it was involved in angiogenesis by binding accumulated succinate in the oxygen-induced retinopathy model [7]. This result has led to speculation that retinal ganglion cells are also a major source of VEGF and a major cellular target for the treatment of the disease. In this study, and in others, we determined that GPR91 was localized to RGCs, cells of the INL, and RPE [7,29,30]. Gnana-Prakasam et al. [29] reported that GPR91 was expressed in RPE, but only in the apical membrane. The increased VEGF expression that was induced by succinate was abolished in RGC-ablated retinas [7], indicating that the succinate-GPR91 receptor may be predominantly expressed in RGCs. Previous research has indicated that intravitreal lentiviral vector administration results in higher transduction efficiency in the inner retina than in the outer retina [31]. Therefore, we used intravitreally administered lentiviral gene transfer technology to explore the role of GPR91 in RGCs in the early stages of DR. Our results showed that GPR91 played an important role in the upregulation of VEGF and retinal vascular dysfunction during the early stages of DR. We considered that increased succinate and activated GPR91 may be the important factors inducing VEGF overexpression in the RGCs.

STZ destroys pancreatic island β cells and is used to induce experimental diabetes in rodents [32]. Adult rats treated with a single dose of STZ exhibit hyperglycemia within 48 h, and these animals are widely used as a model

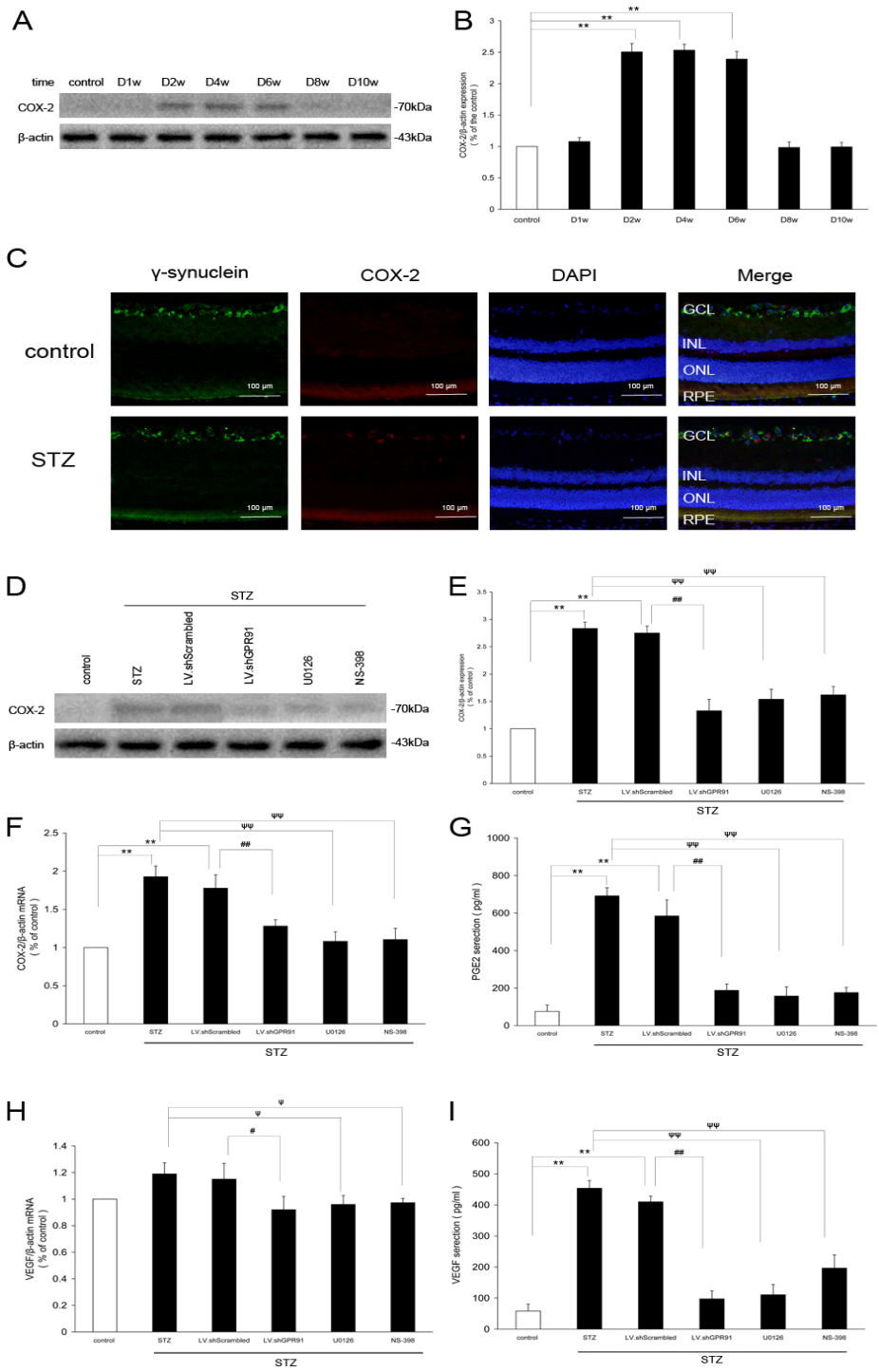

Figure 4. GPR91 modulated VEGF secretion via ERK1/2/cyclooxygenase-2 (COX-2)/ Prostaglandin E_2 (PGE_2) signaling pathway in the retinas of STZ rats. **A**: Western blot analysis of the COX-2 protein in the retinas of diabetic rats in different time periods (from 1 week to 10 weeks). **B**: The levels of COX-2 protein were upregulated in the retinas of diabetic rats during the period of 2 weeks to 6 weeks after the induction of diabetes. Each column denotes the mean ± SD (n = 6). **C**: Immunofluorescence showed that COX-2 expression located in the retinal ganglion cell layer increased in the 4 week diabetic rats compared with the control. Scale bar, 100 μm. **D**: Changes in COX-2 in the retinas of the 4 week diabetic rats treated with scrambled shRNA lentiviral particles, GPR91 shRNA lentiviral particles, 0.1 mM U0126 (ERK1/2 inhibitor), or 0.5 mM NS-398 (COX-2 inhibitor). **E**: The increases in COX-2 expression were significantly blocked by GPR91 shRNA, 0.1 mM U0126 (ERK1/2 inhibitor), or 0.5 mM NS-398 (COX-2 inhibitor). Each column denotes the mean ± SD (n = 6). **F**: qRT-PCR showed that the levels of COX-2 mRNA were decreased obviously in the retinas of the 4 week diabetic rats treated with scrambled shRNA lentiviral particles, GPR91 shRNA lentiviral particles, 0.1 mM U0126 (ERK1/2 inhibitor), or 0.5 mM NS-398 (COX-2 inhibitor) compared with the 4 week diabetic rats. Each column denotes the mean ± SD (n = 6). **G**: Changes in vitreal PGE_2 release in each group. The increase of PGE_2 secretion was significantly blocked by GPR91 shRNA, 0.1 mM U0126 (ERK1/2 inhibitor), or 0.5 mM NS-398 (COX-2 inhibitor) in the retinas of 4 week diabetic rats. Each column denotes the mean ± SD (n = 6). **H**: The levels of VEGF mRNA (using qRT-PCR) were downregulated in the 4 week diabetic rats treated with GPR91 shRNA, 0.1 mM U0126 (ERK1/2 inhibitor), or 0.5mM NS-398 (COX-2 inhibitor) compared with the STZ rats. Each column denotes the mean ± SD (n = 6). **I**: Enzyme-linked immunosorbent assay analysis of vitreal VEGF release in vitreous. The increase of VEGF secretion was significantly blocked in the 4 week diabetic rats treated with GPR91 shRNA, 0.1 mM U0126 (ERK1/2 inhibitor), or 0.5 mM NS-398 (COX-2 inhibitor) compared with the 4 week diabetic rats. Each column denotes the mean ± SD (n = 6). **p<0.01 versus control. #p<0.05 versus LV.shScrambled group rats. ##p<0.01 versus LV.shScrambled group rats. ψ<0.05 versus STZ group rats. ψψ<0.01 versus STZ group rats.

of insulin-dependent diabetes. The induction of diabetes with STZ is associated with hyperglycemia and significant weight loss. In our experiments, no supplemental insulin was administered to prevent weight loss. Our results found that the intravitreal injection of GPR91 shRNA lentiviral particles had no effect on hyperglycemia or weight loss in the diabetic animals, suggesting that the effects of GPR91 shRNA on retinal VEGF expression and vascular dysfunction are most likely mediated by a local mechanism rather than by a systemic mechanism. In this study, we demonstrated retinal telangiectatic vessels, a thickened capillary basement membrane, and vascular leakage as determined by assessing ultrastructural changes and performing Evans blue dye permeability studies in STZ-induced diabetic rats. Our results were similar to the reports of Zhang et al., who investigated VEGF upregulation and retinal vascular dysfunction during the process of DR [33]. Numerous studies have reported that VEGF is a potent factor involved in the induction of retinal permeability [6,34]. Additionally, our previous in vitro study demonstrated that VEGF was involved in the proliferation and migration of endothelial cells [15]. Kaur et al. demonstrated that the inner retinal barrier, which is associated with the tight junctions between the neighboring retinal capillary endothelial cells, was more sensitive to hypoxia and ischemia than the outer retinal barrier [35]. We concluded that this vascular leakage was due to an inner retinal barrier dysfunction, but the data do not exclude the possibility of an outer retinal barrier dysfunction [15]. Meanwhile, we also found that lentiviral-delivered GPR91 shRNA attenuated these dysfunctions in the retinal vasculature significantly, but GPR91 had no effect on the damage of the inner nuclear layer during the development of DR. These results suggested that in the retinal ganglion layer, GPR91 may modulate retinal vascular dysfunction by regulating VEGF expression in the retina. In our study, the mRNA levels of VEGF did not parallel the protein levels of VEGF; therefore, we speculated that there were temporal and spatial differences in gene transcription and translation. First, the time of the VEGF mRNA peak may be earlier than that of the VEGF protein level peak. Second, different regulation mechanisms, acting on both the synthesized mRNA and the synthesized protein, can differentially affect the relative amounts of the two molecules. Finally, there are many well studied molecular processes, such as post-transcription processing and degradation of transcription products, that can affect the relative amounts of mRNA and protein.

The present study demonstrated that succinate accumulated in the retina during the early stages of diabetes, which was consistent with the results in the kidney [10]. Succinate, as an intermediate of the Krebs cycle, is produced by the oxidation of succinyl-CoA by the enzyme succinyl-CoA hydrolase and is further oxidized to fumarate by succinate dehydrogenase [9]. The activity of the Krebs cycle is regulated to match metabolic demands, but pathological situations such as ischemia and hyperglycemia can disrupt the flow of substrates in this cycle, resulting in increased succinate levels [7,10]. Succinate has received intense attention for its role in cellular signaling events via its specific receptor GPR91 [8]. Thus far, reports have demonstrated that succinate-induced activation of GPR91 mutiple biological signals change including Ca^{2+}, PKA-dependent pathway[12], NO , COX-2 and renin-angiotensin system [10,23] in various tissues. Earlier studies showed that the MAPK signaling pathways are activated by G protein-coupled receptors [36,37]. This study indicates that succinate, via its receptor GPR91 in RGCs, mediates the ERK1/2/COX-2/PGE_2 signaling pathway activation and results in the increase of the angiogenic factor VEGF during the pathological process in STZ-induced diabetic retinopathy (Figure 5).

ERK1/2 signaling is associated with many cellular responses, such as proliferation, differentiation, and development [38]. However, this pathway's inappropriate and continuous activation contributed to oncogenesis [38], diabetic complications [39], and angiogenesis [40]. In the retinopathy of prematurity (ROP) model, ERK1/2 was found to be involved in VEGF-induced retinal microvascular endothelial cell proliferation [41]. Our research showed that VEGF release was obviously reduced by using ERK1/2 inhibitor U0126 in the STZ-induced diabetic rats. U0126 is widely thought to act as a potent ERK1/2 antagonist to induce DR pathology [42]. This finding suggested that ERK1/2 played an important role in the process of DR. ERK1/2 kinases belong to a large family of serine/threonine kinases that are triggered by multiple extracellular signals and ERK1/2 kinases transfer the information within the cells. Activation of ERK1/2 is associated with dual phosphorylation of the protein kinase activating loop on threonine and tyrosine residues [20]. The ERK1/2 pathways are tightly regulated by and cross-communicate with the other signaling pathways involved in a wide variety of tissues, such as cAMP, PKC, RTK, and TNF-β and PI3K [38]. In our studies, we demonstrated that the ERK1/2-induced VEGF secretion, at least partially, was regulated by GPR91 in DR.

COX-2 has been intensely studied for many years as an inflammatory mediator, and the upregulation of COX-2 expression has been suggested to lead to inflammation during the development of diabetic retinopathy [43]. Recent research demonstrated that inflammation contributes to local ischemia in the retina and further induces pathological angiogenesis

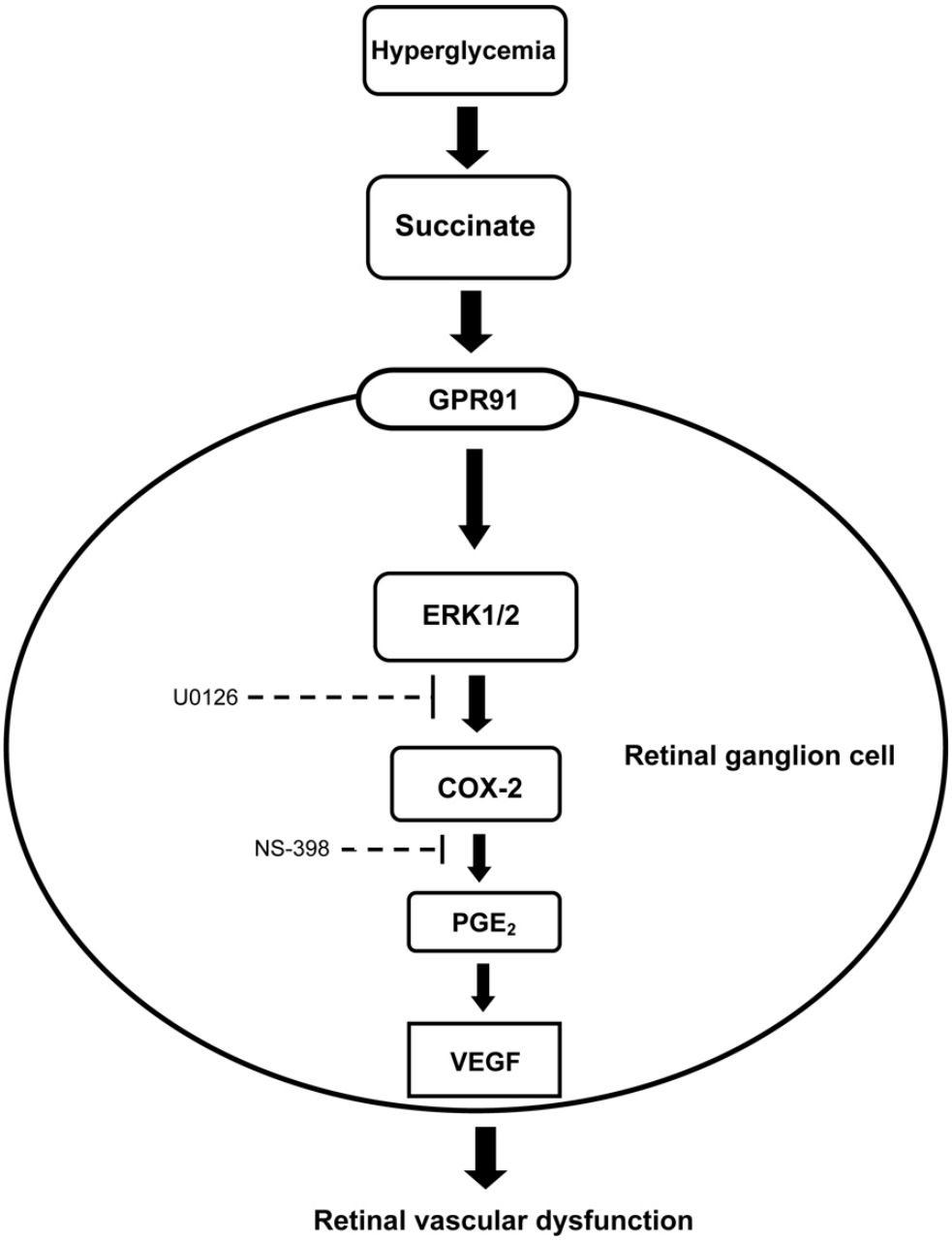

Figure 5. Succinate and the GPR91 signaling pathway in the retinas of STZ-induced diabetic rats. Each *solid line and arrow* denotes a step in an activating pathway. Succinate accumulation triggered by hyperglycemia activates GPR91 signaling, sequentially activating ERK1/2 and then upregulating COX-2 and PGE_2 expression, and later increasing VEGF release in retinal ganglion cells. The increase of VEGF induces retinal vascular dysfunction and plays a key role in the pathology of diabetic retinopathy. The *long dashed line and vertical lines* denotes a step in an inhibiting pathway. U0126 blocks the ERK1/2 signaling pathway and the downstream expression of COX-2, PGE_2, and VEGF. NS-398 blocks COX-2 and PGE_2 and decreases PGE_2-mediated VEGF synthesis.

[44,45]. Moreover, data have shown that increased levels of COX-2 are associated with the upregulation of VEGF in various tissues [46-48]. Our results, as described in this report, are similar to those of these studies. Some research showed that the MAPK signaling pathway was involved in the activation of COX-2 [49,50]. Before our studies, the exact signals that mediated the increase in COX-2 in DR were unknown. PGE_2, an important COX-2 product, is also a strong inducer of VEGF in cells, including rheumatoid synovial fibroblasts [51], human monocytic THP-1 cells [52], and Müller cells [53]. Our findings now have identified the metabolic receptor GPR91 as a strong candidate for the underlying signaling mechanism of COX-2 in the early stages of DR. The results of our investigation also established that ERK1/2 phosphorylation, COX-2, and VEGF are upregulated in parallel, and this upregulation partially relies on the activation of GPR91. Additional studies using the ERK1/2 inhibitor U0126 and COX-2 inhibitor NS-398 abolished COX-2, PGE_2 production, and VEGF secretion, providing further confirmation that ERK1/2 and ERK1/2-dependent COX-2 and PGE_2 are involved in GPR91-dependent succinate-induced VEGF release. On the basis of the findings from

this study, a working signaling model of the succinate and GPR91 signaling pathway occurring in retinal ganglion cells is proposed (Figure 5). Despite promising results, it is not clear that the GPR91 receptor is exclusively responsible for the observed effects because shGPR91 only knocks down the expression of GPR91 instead of knocking it out or silencing it completely. Studies with GPR91 knockout mice and GPR91 overexpression studies would help to clarify this point.

In conclusion, we demonstrated that the retinal vascular dysfunction caused by accumulated succinate and the activity of GPR91 was dependent on ERK1/2 signaling, COX-2 and PGE_2 expression and subsequently increased secretion of VEGF in the early stages of DR. We cannot completely rule out other mechanisms of DR because there may be several intricate signaling pathways involved. However, these observations provide a basis for future investigations concerning the potential therapeutic implications of GPR91-dependent signaling-related inhibitors in inhibiting the development of DR.

ACKNOWLEDGMENTS

This work was supported by grants from the Research Fund for the National Natural Science Foundation of China (No. 81070738) and the Key Basic Science Foundation of Science and Technology Commission of Shanghai Manicipality (No. 11JC1407702). No potential conflicts of interest relevant to this article were reported.

REFERENCES

1. Ibrahim AS, El-Shishtawy MM, Zhang W, Caldwell RB, Liou GIA. ((2)A) adenosine receptor (A((2)A)AR) as a therapeutic target in diabetic retinopathy. Am J Pathol 2011; 178:2136-45. [PMID: 21514428].
2. Wu H, Jiang C, Gan D, Liao Y, Ren H, Sun Z, Zhang M, Xu G. Different effects of low- and high-dose insulin on ROS production and VEGF expression in bovine retinal microvascular endothelial cells in the presence of high glucose. Graefes Arch Clin Exp Ophthalmol 2011; 249:1303-10. [PMID: 21494874].
3. Kim J, Kim CS, Lee YM, Jo K, Shin SD, Kim JS. Methylglyoxal induces hyperpermeability of the blood-retinal barrier via the loss of tight junction proteins and the activation of matrix metalloproteinases. Graefes Arch Clin Exp Ophthalmol 2012; 250:691-7. [PMID: 22249316].
4. Praidou A, Papakonstantinou E, Androudi S, Georgiadis N, Karakiulakis G, Dimitrakos S. Vitreous and serum levels of vascular endothelial growth factor and platelet-derived growth factor and their correlation in patients with non-proliferative diabetic retinopathy and clinically significant macula oedema. Acta Ophthalmol (Copenh) 2011; 89:248-54. [PMID: 19799585].
5. Yuan D, Yuan D, Liu Q. Association of the receptor for advanced glycation end products gene polymorphisms with diabetic retinopathy in type 2 diabetes: a meta-analysis. Ophthalmologica 2012; 227:223-32. [PMID: 22354095].
6. Witmer AN, Blaauwgeers HG, Weich HA, Alitalo K, Vrensen GF, Schlingemann RO. Altered expression patterns of VEGF receptors in human diabetic retina and in experimental VEGF-induced retinopathy in monkey. Invest Ophthalmol Vis Sci 2002; 43:849-57. [PMID: 11867607].
7. Sapieha P, Sirinyan M, Hamel D, Zaniolo K, Joyal JS, Cho JH, Honoré JC, Kermorvant-Duchemin E, Varma DR, Tremblay S, Leduc M, Rihakova L, Hardy P, Klein WH, Mu X, Mamer O, Lachapelle P, Di Polo A, Beauséjour C, Andelfinger G, Mitchell G, Sennlaub F, Chemtob S. The succinate receptor GPR91 in neurons has a major role in retinal angiogenesis. Nat Med 2008; 14:1067-76. [PMID: 18836459].
8. He W, Miao FJ, Lin DC, Schwandner RT, Wang Z, Gao J, Chen JL, Tian H, Ling L. Citric acid cycle intermediates as ligands for orphan G-protein-coupled receptors. Nature 2004; 429:188-93. [PMID: 15141213].
9. Correa PR, Kruglov EA, Thompson M, Leite MF, Dranoff JA, Nathanson MH. Succinate is a paracrine signal for liver damage. J Hepatol 2007; 47:262-9. [PMID: 17451837].
10. Toma I, Kang JJ, Sipos A, Vargas S, Bansal E, Hanner F, Meer E, Peti-Peterdi J. Succinate receptor GPR91 provides a direct link between high glucose levels and renin release in murine and rabbit kidney. J Clin Invest 2008; 118:2526-34. [PMID: 18535668].
11. Matsumoto M, Suzuma K, Maki T, Kinoshita H, Tsuiki E, Fujikawa A, Kitaoka T. Succinate increases in the vitreous fluid of patients with active proliferative diabetic retinopathy. Am J Ophthalmol 2012; 153:896-902. [PMID: 22265145].
12. Aguiar CJ, Andrade VL, Gomes ER, Alves MN, Ladeira MS, Pinheiro AC, Gomes DA, Almeida AP, Goes AM, Resende RR, Guatimosim S, Leite MF. Succinate modulates Ca2+ transient and cardiomyocyte viability through PKA-dependent pathway. Cell Calcium 2012; 47:37-46. .
13. Rubic T, Lametschwandtner G, Jost S, Hinteregger S, Kund J, Carballido-Perrig N, Schwärzler C, Junt T, Voshol H, Meingassner JG, Mao X, Werner G, Rot A, Carballido JM. Triggering the succinate receptor GPR91 on dendritic cells enhances immunity. Nat Immunol 2008; 9:1261-9. [PMID: 18820681].
14. Robben JH, Fenton RA, Vargas SL, Schweer H, Peti-Peterdi J, Deen PM, Milligan G. Localization of the succinate receptor in the distal nephron and its signaling in polarized MDCK cells. Kidney Int 2009; 76:1258-67. [PMID: 19776718].
15. Hu J, Wu Q, Li T, Chen Y, Wang S. Inhibition of high glucose-induced VEGF release in retinal ganglion cells by RNA interference targeting G protein-coupled receptor 91. Exp Eye Res 2013; 109:31-9. [PMID: 23379999].
16. Ayalasomayajula SP, Amrite AC, Kompella UB. Inhibition of cyclooxygenase-2, but not cyclooxygenase-1, reduces prostaglandin E2 secretion from diabetic rat retinas. Eur J Pharmacol 2004; 498:275-8. [PMID: 15364005].

17. Raman M, Chen W, Cobb MH. Differential regulation and properties of MAPKs. Oncogene 2007; 26:3100-12. [PMID: 17496909].

18. Seger R, Krebs EG. The MAPK signaling cascade. FASEB J 1995; 9:726-35. [PMID: 7601337].

19. Kamal A, Faazil S, Ramaiah MJ, Ashraf M, Balakrishna M, Pushpavalli SN, Patel N, Pal-Bhadra M. Synthesis and study of benzothiazole conjugates in the control of cell proliferation by modulating Ras/MEK/ERK-dependent pathway in MCF-7 cells. Bioorg Med Chem Lett 2013; 23:5733-9. [PMID: 23999041].

20. Berra E, Pages G, Pouysse'gur J. MAP kinases and hypoxia in the control of VEGF expression. Cancer Metastasis Rev 2000; 19:139-45. [PMID: 11191053].

21. Lee JJ, Hsiao CC, Yang IH, Chou MH, Wu CL, Wei YC, Chen CH, Chuang JH. High-mobility group box 1 protein is implicated in advanced glycation end products-induced vascular endothelial growth factor A production in the rat retinal ganglion cell line RGC-5. Mol Vis 2012; 18:838-50. [PMID: 22511847].

22. Ye X, Ren H, Zhang M, Sun Z, Jiang AC, Xu G. ERK1/2 signaling pathway in the release of VEGF from Müller cells in diabetes. Invest Ophthalmol Vis Sci 2012; 53:3481-9. [PMID: 22511624].

23. Vargas SL, Toma I, Kang JJ, Meer EJ, Peti-Peterdi J. Activation of the succinate receptor GPR91 in macula densa cells causes renin release. J Am Soc Nephrol 2009; 20:1002-11. [PMID: 19389848].

24. Zhang X, Bao S, Lai D, Rapkins RW, Gillies MC. Intravitreal triamcinolone acetonide inhibits breakdown of the blood-retinal barrier through differential regulation of VEGF-A and its receptors in early diabetic rat retinas. Diabetes 2008; 57:1026-33. [PMID: 18174522].

25. Moravski CJ, Kelly DJ, Cooper ME, Gilbert RE, Bertram JF, Shahinfar S, Skinner SL, Wilkinson-Berka JL. Retinal neovascularization is prevented by blockade of the renin-angiotensin system. Hypertension 2000; 36:1099-104. [PMID: 11116132].

26. Zheng Z, Chen H, Li J, Li T, Zheng B, Zheng Y, Jin H, He Y, Gu Q, Xu X. Sirtuin 1-mediated cellular metabolic memory of high glucose via the LKB1/AMPK/ROS pathway and therapeutic effects of metformin. Diabetes 2012; 61:217-28. [PMID: 22124463].

27. Xu Q, Qaum T, Adamis AP. Sensitive blood-retinal barrier breakdown quantitation using Evans blue. Invest Ophthalmol Vis Sci 2001; 42:789-94. [PMID: 11222542].

28. Wang J, Xu X, Elliott MH, Zhu M, Le YZ. Muller cell-derived VEGF is essential for diabetes-induced retinal inflammation and vascular leakage. Diabetes 2010; 59:2297-305. [PMID: 20530741].

29. Gnana-Prakasam JP, Ananth S, Prasad PD, Zhang M, Atherton SS, Martin PM, Smith SB, Ganapathy V. Expression and iron-dependent regulation of succinate receptor GPR91 in retinal pigment epithelium. Invest Ophthalmol Vis Sci 2011; 52:3751-8. [PMID: 21357408].

30. Favret S, Binet F, Leboeuf D, Carbadillo J, Rubic T, Picard E, Mawambo G, Tetreault N, Joyal JS, Chemtob S, Sennlaub F, Sangiovanni JP, Guimond M, Sapieha P. Deficiency in the metabolite receptor SUCNR1 (GPR91) leads to outer retinal lesions. Aging (Albany, NY Online) 2013; 5:427-44. [PMID: 23833031].

31. Auricchio A, Kobinger G, Anand V, Hildinger M, O'Connor E, Maguire AM, Wilson JM, Bennett J. Exchange of surface proteins impacts on viral vector cellular specificity and transduction characteristics: the retina as a model. Hum Mol Genet 2001; 10:3075-81. [PMID: 11751689].

32. Kusari J, Zhou S, Padillo E, Clarke KG, Gil DW. Effect of memantine on neuroretinal function and retinal vascular changes of streptozotocin-induced diabetic rats. Invest Ophthalmol Vis Sci 2007; 48:5152-9. [PMID: 17962468].

33. Zhang W, Yan H. Dysfunction of circulating endothelial progenitor cells in type 1 diabetic rats with diabetic retinopathy. Graefes Arch Clin Exp Ophthalmol 2013; 251:1123-31. [PMID: 23385543].

34. Tong N, Zhang Z, Zhang W, Qiu Y, Gong Y, Yin L, Qiu Q, Wu X. Diosmin alleviates retinal edema by protecting the blood-retinal barrier and reducing retinal vascular permeability during ischemia/reperfusion injury. PLoS ONE 2013; 8:e61794-[PMID: 23637907].

35. Kaur C, Sivakumar V, Yong Z, Lu J, Foulds WS, Ling EA. Blood-retinal barrier disruption and ultrastructural changes in the hypoxic retina in adult rats: the beneficial effect of melatonin administration. J Pathol 2007; 212:429-39. [PMID: 17582234].

36. Schulte G, Fredholm BB. Human adenosine A(1), A(2A), A(2B), and A(3) receptors expressed in Chinese hamster ovary cells all mediate the phosphorylation of extracellular-regulated kinase 1/2. Mol Pharmacol 2000; 58:477-82. [PMID: 10953039].

37. Yoon S, Seger R. The extracellular signal-regulated kinase: multiple substrates regulate diverse cellular functions. Growth Factors 2006; 24:21-44. [PMID: 16393692].

38. Zhang W, Liu HT. MAPK signal pathways in the regulation of cell proliferation in mammalian cells. Cell Res 2002; 12:9-18. [PMID: 11942415].

39. Tan Y, Ichikawa T, Li J, Si Q, Yang H, Chen X, Goldblatt CS, Meyer CJ, Li X, Cai L, Cui T. Diabetic downregulation of Nrf2 activity via ERK contributes to oxidative stress-induced insulin resistance in cardiac cells in vitro and in vivo. Diabetes 2011; 60:625-33. [PMID: 21270272].

40. Nakabayashi H, Shimizu K. HA1077, a Rho kinase inhibitor, suppresses glioma-induced angiogenesis by targeting the Rho-ROCK and the mitogen-activated protein kinase kinase/extracellular signal-regulated kinase (MEK/ERK) signal pathways. Cancer Sci 2011; 102:393-9. [PMID: 21166955].

41. Bullard LE, Qi X, Penn JS. Role for extracellular signal-responsive kinase-1 and −2 in retinal angiogenesis. Invest Ophthalmol Vis Sci 2003; 44:1722-31. [PMID: 12657614].

42. Mohammad G, Mairaj Siddiquei M, Imtiaz Nawaz M, Abu El-Asrar AM. The ERK1/2 Inhibitor U0126 Attenuates Diabetes-Induced Upregulation of MMP-9 and Biomarkers of Inflammation in the Retina. J Diabetes Res 2013; 2013:658548-[PMID: 23671886].

43. Kern TS. Contributions of inflammatory processes to the development of the early stages of diabetic retinopathy. Exp Diabetes Res 2007; 2007:95103-[PMID: 18274606].

44. Neroev VV, Zueva MV, Kalamkarov GR. Molecular mechanisms of retinal ischemia. Vestn Oftalmol 2010; 126:59-64. [PMID: 20608206].

45. Patel N. Targeting leukostasis for the treatment of early diabetic retinopathy. Cardiovasc Hematol Disord Drug Targets 2009; 9:222-9. [PMID: 19619127].

46. Nagoya H, Futagami S, Shimpuku M, Tatsuguchi A, Wakabayashi T, Yamawaki H, Kodaka Y, Kawagoe T, Watarai Y, Makino H, Miyashita M, Tsuchiya S, Crowe SE, Sakamoto C. Apurinic/apyrimidinic endonuclease-1 is associated with angiogenesis and VEGF production via upregulation of COX-2 expression in esophageal cancer tissues. Am J Physiol Gastrointest Liver Physiol 2014; 306:G183-90. [PMID: 24284961].

47. Xin X, Majumder M, Girish GV, Mohindra V, Maruyama T, Lala PK. Targeting COX-2 and EP4 to control tumor growth, angiogenesis, lymphangiogenesis and metastasis to the lungs and lymph nodes in a breast cancer model. Lab Invest 2012; 92:1115-28. [PMID: 22641101].

48. Zhou LH, Hu Q, Sui H, Ci SJ, Wang Y, Liu X, Liu NN, Yin PH, Qin JM, Li Q. Tanshinone II–a inhibits angiogenesis through down regulation of COX-2 in human colorectal cancer. Asian Pac J Cancer Prev 2012; 13:4453-8. [PMID: 23167360].

49. Peti-Peterdi J. High glucose and renin release: the role of succinate and GPR91. Kidney Int 2010; 78:1214-7. [PMID: 20861827].

50. Ulivi V, Giannoni P, Gentili C, Cancedda R, Descalzi F. p38/NF-kB-dependent expression of COX-2 during differentiation and inflammatory response of chondrocytes. J Cell Biochem 2008; 104:1393-406. [PMID: 18286508].

51. Inoue H, Takamori M, Nagata N, Nishikawa T, Oda H, Yamamoto S, Koshihara Y. An investigation of cell proliferation and soluble mediators induced by interleukin 1beta in human synovial fibroblasts: comparative response in osteoarthritis and rheumatoid arthritis. Inflamm Res 2001; 50:65-72. [PMID: 11289656].

52. Höper MM, Voelkel NF, Bates TO, Allard JD, Horan M, Shepherd D, Tuder RM. Prostaglandins induce vascular endothelial growth factor in a human monocytic cell line and rat lungs via cAMP. Am J Respir Cell Mol Biol 1997; 17:748-56. [PMID: 9409562].

53. Cheng T, Cao W, Wen R, Steinberg RH, LaVail MM. Prostaglandin E2 induces vascular endothelial growth factor and basic fibroblast growth factor mRNA expression in cultured rat Muller cells. Invest Ophthalmol Vis Sci 1998; 39:581-91. [PMID: 9501870].

Articles are provided courtesy of Emory University and the Zhongshan Ophthalmic Center, Sun Yat-sen University, P.R. China. The print version of this article was created on 31 July 2014. This reflects all typographical corrections and errata to the article through that date. Details of any changes may be found in the online version of the article.